

Light extraction enhancement from nano-imprinted photonic crystal GaN-based blue light-emitting diodes

Hyun Kyong Cho^{a)}, Junho Jang, Jeong-Hyeon Choi, Jaewan Choi,
Jongwook Kim, Jeong Soo Lee

LED R&D Lab, LG Electronics Institute of Technology, Seoul 137-724, Korea
hkcho@lge.com

Beomseok Lee, Young Ho Choe, Ki-Dong Lee, Sang Hoon Kim, Kwiro Lee

Device and Materials Lab, LG Electronics Institute of Technology, Seoul 137-724, Korea

Sun-Kyung Kim, Yong-Hee Lee

Department of Physics, Korea Advanced Institute of Science and Technology, Taejon 305-701, Korea

Abstract: The nano-imprint lithography method was employed to incorporate wide-area ($375 \times 330 \mu\text{m}^2$) photonic-crystal (PC) patterns onto the top surface of GaN-based LEDs. When the 280-nm-thick *p*-GaN was partly etched to $\sim 140\text{nm}$, the maximal extraction-efficiency was observed without deteriorating electrical properties. After epoxy encapsulation, the light output of the PC LED was enhanced by 25% in comparison to the standard LED without pattern, at a standard current of 20mA. By three-dimensional finite-difference time-domain method, we found that the extraction efficiency of the LED tends to be saturated as the etch-depth in the GaN epitaxial-layer becomes larger than the wavelength of the guided modes.

©2005 Optical Society of America

OCIS codes: (230.3670) Light-emitting diodes; (160.6000) Semiconductors, including MQW; (2230.3740) Lithography

References and links

1. A. David, T. Fujii, R. Sharma, K. McGroody, S. Nakamura, S. P. DenBaars, E. L. Hu, and C. Weisbuch, "Photonic-crystal GaN light-emitting diodes with tailored guided mode distribution," *Appl. Phys. Lett.* **88**, 061124 (2006).
2. E. Stefanov, B. S. Shelton, H. S. Venugopalan, T. Zhang, and I. Eliashevich, "Optimizing the external light extraction of nitride LEDs," in *Solid State Lighting II*, I. T. Ferguson, N. Narendran, S. P. DenBaars, Y.-S. Park, eds., Proc. SPIE **4776**, 223 234 (2002).
3. Y. C. Chen, J. J. Wierer, M. R. Krames, M. J. Ludowise, M. S. Misra, F. Ahmed, A. Y. Kim, G. O. Mueller, J. C. Bhat, S. A. Stockman, and P. S. Martin, "Optical cavity effects in InGaN/GaN quantum-well-heterostructure flip-chip light-emitting diodes," *Appl. Phys. Lett.* **82**, 2221 (2003).
4. Y. J. Lee, S. H. Kim, J. Huh, G. H. Kim, Y. H. Lee, S. H. Cho, Y. C. Kim, and Y. R. Do, "A high-extraction-efficiency nanopatterned organic light-emitting diode," *Appl. Phys. Lett.* **82**, 3779 (2003).
5. K. Okamoto, I. Niki, A. Shvartster, Y. Narukawa, T. Mukai, and A. Scherer, *Nature* **3**, 601 (2004).
6. Y. N. Oder, K. H. Kim, J. Y. Lin, and H. X. Jiang, "III-nitride blue and ultraviolet photonic crystal light emitting diodes," *Appl. Phys. Lett.* **84**, 466 (2004).
7. L. Chen, and A. V. Nurmikko, "Fabrication and performance of efficient blue light emitting III-nitride photonic crystals," *Appl. Phys. Lett.* **85**, 3663 (2004).
8. A. David, C. Meier, R. Sharma, F. S. Diana, S. P. DenBaars, E. Hu, S. Nakamura, and C. Weisbuch, "Photonic bands in two-dimensionally patterned multimode GaN waveguides for light extraction," *Appl. Phys. Lett.* **87**, 101107 (2005).
9. W. S. Wong, T. Sands, N. W. Cheung, M. Kneissl, D. P. Bour, P. Mei, L. T. Romando, and N. M. Johnson, "Fabrication of thin-film InGaN light-emitting diode membranes by laser lift-off," *Appl. Phys. Lett.* **75**, 1360 (1999)

10. D. H. Kim, C. O. Cho, Y. G. Roh, H. Jeon, Y. S. Park, J. Cho, J. S. Im, C. Sone, Y. Park, W. J. Choi, and Q-Han Park, "Enhanced light extraction from GaN-based light-emitting diodes with holographically generated two-dimensional photonic crystal patterns," *Appl. Phys. Lett.* **87**, 203508 (2005)
11. The issue on the lattice constant will be described in the other paper.
12. L Jay Guo, "Recent progress in nanoimprint technology and its applications," *J. Phys. D Appl. Phys.* **37**, R123 (2004)

1. Introduction

GaN-based light-emitting diodes (LEDs) have been employed for various applications, including traffic signals, full-color displays, back light units for liquid-crystal display and so forth. Likewise other conventional semiconductor LEDs, the high refractive index of GaN ($n=2.46$) prohibits light beyond a critical angle (θ_c) from being extracted because of the phase-mismatch. For instance, the ratio of the total flux reaching the capping layer filled with epoxy ($n=1.4$) through the top GaN surface upon the first reflection is merely $\int_0^{\theta_c} (1-r(\theta))^2 \sin \theta d\theta = 15.4\%$, where $r(\theta)$ is the Fresnel reflection coefficient. This value covers the light going downward initially and then reflecting back at a mirror beneath the sapphire substrate. Certainly, if one wishes to define the extraction efficiency rigorously, one should also consider the horizontal radiation through four side-facets surrounding the LED [1]. Typically, the amount of photons escaping through the side-facets of GaN layer can be negligible for large-area LEDs, because the active material in the GaN LED has a fairly large extinction-coefficient ($k \sim 0.05$) [2]. In comparison, the transmission through the side-facets of the non-absorbing, sapphire-substrate contributes more to the horizontal radiation. In most schemes, the amount of the horizontal radiation is almost constant and it may not be a matter of main concern. Thus, considering the total portion of the extracted light, one can urge that there are still a plenty of rooms of improvement for the light extraction.

There have been two basic schemes toward the high-efficiency of GaN LED. One is to directly manipulate the physical properties (radiation pattern and decay-time) of the light source by the microcavity effect [3, 4, 5]. In this case, a highly reflective metal is placed close to the light-emitting element. The other is to incorporate nanopatterns to convert the guided waves trapped in an epoxy-GaN-sapphire multimode waveguide into external leaky waves [6,7,8]. The former scheme is available only for flip chips or laser lift-off GaN LEDs [9]. Although a number of attempts incorporating the photonic crystal (PC) into various LEDs have been reported, the effect of the etch-depth on the light extraction was not investigated thoroughly. In this study, we focused on the etch-depth for maximum extraction efficiency, employing PC patterns on the top surface of the GaN LED. Computationally, we employed the three-dimensional finite-difference time-domain (3D-FDTD) method. This analysis shows the escape route of the light generated in LEDs into the capping layer for a given time.

From the viewpoint of practical manufacturing, the fabrication of the sub-micron feature has been the nontrivial issue [10]. So far, the wavelength-scale patterns have been mostly defined by the electron-beam lithography. Here, we tried nano-imprint lithography (NIL) techniques to define large-area PC patterns ($375 \times 330 \mu\text{m}^2$) for the PC GaN-LEDs. For comparison purposes, we prepared GaN LEDs of various PCs with different etch-depths. The relative enhancement in light output was measured by an integration-sphere setup after epoxy encapsulation

2. Fabrication of PC GaN LEDs by Nano-imprint Lithography

The GaN-based LED structures were grown on sapphire substrates by metal organic chemical vapor deposition. The schematic of the PC GaN-LED is shown in Fig. 1(a). On the bottom sapphire substrate, the LED structure consists of a low-temperature GaN buffer layer, a $2 \mu\text{m}$ -thick undoped GaN layer, a $3 \mu\text{m}$ -thick Si-doped n -type GaN layer, followed by $0.1 \mu\text{m}$ -thick InGaN/GaN multiple-quantum-well (MQW) layers and a $0.3 \mu\text{m}$ -thick Mg-doped p -type GaN. Prior to defining PC patterns, a 2800\AA transparent indium tin oxide (ITO) film was deposited

by sputtering process. After standard fabrication steps for normal LED devices ($375 \times 330 \mu\text{m}^2$), two-dimensional square-lattice air-hole arrays with a lattice constant of 1200nm are formed by NIL techniques [11]. The NIL is essentially a micro-molding process in which the topography of a template defines the patterns on a substrate [12]. The resolution of the NIL is limited by that of the template. This process promises important advantages in manufacturing over photolithography and other lithography techniques. Note that the NIL does not require expensive projection optics, advanced illumination sources, or specialized resist materials that are the central to the others. The NIL is especially suitable for large-area processing.

In order to generate patterns on ITO/GaN, a SiO_2 thin film layer and a Cr metal layer were used as etch masks. These layers were deposited by sputtering process. Finally, ITO and GaN layers were etched using inductively coupled plasma reactive ion etching with CH_4 and BCl_3/Cl_2 , respectively as shown in Fig. 1(b).

3. Computation of extraction-efficiency with various etch-depths

As aforementioned, the total internal reflection (TIR) prevents LED devices from gaining high-efficiency. The TIR is attributed to the mismatch of the in-plane directional momentum of light when $\theta > \theta_c$. Generally, the periodic PC pattern can add (or subtract) the Bloch momentum to photons such that they can penetrate into a lower index medium; otherwise, the trapped photons become extinct through the absorption. Since the absorption losses are unavoidable, it is important to find ways to turn the guided modes into leaky continuum modes before they are lost.

To design the adequate PC structure promising high extraction efficiency, one generally has to consider various parameters such as lattice constant, the type of lattice, filling-factor, and etch-depth. Among parameters described here, we paid a special attention to the effect of the etch-depth. To compute the extraction efficiency as a function of the etch-depth, we used the 3D-FDTD method. Although the 3D-FDTD simulations enables us to acquire accurate results for the small-size model structure, the large-area GaN-LED cannot be treated faithfully because of the limited memory size. In our computation, the structure is simplified to fit within the finite memory of the computer (2-Gbyte) [Fig. 2(a)]. Specifically, the thickness of the sapphire substrate is shrunk down to $1.5 \mu\text{m}$ (from a few-hundreds micron in the original one) and the total thickness of GaN epitaxial-layer is set to be $3.0 \mu\text{m}$. The transverse size is around $12 \mu\text{m}$ which is much less than that of the real device. However, by placing the perfect-mirror with reflectance of 100% at four sides of the structure, we could mimic light that is propagating indefinitely. To represent MQWs in the GaN LED, randomly polarized dipole sources are placed at a depth of 330nm from the top GaN surface, which corresponds to the middle of the MQWs. Because the dipole sources are placed from the perfect mirrors distantly, the modification of the angular emission pattern by coherent reflections between the perfect mirrors is negligible. The center wavelength of the dipole source is 450nm and the spectral width (as a full-width half-maximum) is 30nm. The thickness of ITO and *p*-GaN are 300nm and 280nm, respectively. The outer medium is epoxy and its refractive index is 1.4. Figure 2(a) (up and bottom) shows the snap shots of the electric-field distribution after the sources are extinguished. Here, the extraction efficiency is defined as a ratio of the vertically-extracted energy through the top GaN surface and the total generated energy. For simplicity, the optical absorptions of the constituent materials are ignored. The extraction efficiency is plotted as a function of the propagation-distance of light for several etch-depths [Fig. 2(b)]. In all cases, the lattice constant (a) is fixed at 1080nm and the radii of holes are $0.30a$ (a filling-factor $f=0.28$). Note in Fig. 2(c) that our choice of the lattice constant (1080nm) is away from the optimum ($\sim 700\text{nm}$). However, we tried the larger structure, because it is easier to fabricate with high fidelity by employing our NIL technology. Additionally, we decided to focus on the effect of the etch depth. For the normal GaN LED with the planar surface, the efficiency begins to increase initially. However, after one round trip, it almost saturates around 8%, which is nearly identical to the value taken by the analytical way. On the other hand, the PC GaN-LEDs exhibit the steady increase of the efficiency with the propagation distance. In this

case, the light can have additional opportunities to be coupled to leaky modes after successive reflection. As the etch-depth becomes deeper, the rate of energy extraction becomes larger. This tendency on the etch-depth is maintained regardless of the lattice constant, except that the increase rate of the energy extraction with the etch-depths is different. To attain the high extraction efficiency, it is essential to etch the GaN layer sufficiently. When the etch-depth in the GaN layer is too shallow, the lower-order guided modes occupying relatively large portion can hardly feel the presence of the PCs [1]. However, as the etch-depth in GaN layer becomes comparable to the wavelength of the guided modes ($\sim\lambda/n$, n is the effective index of the guided modes), the extraction-efficiency increases significantly. The increment of the extraction-efficiency is reduced little by little as the etch-depth is deeper than $\sim\lambda/n$. Lastly, the extraction-efficiency converges to a certain value when the total etch-depth in the GaN-layer reaches around 450nm. This implies that the guided modes feel the deeply-etched PC partly as a new intermediate layer having an effective index set by the filling-factor. The emergence of the intermediate layer shifts the field distribution of the guided-modes downward such that they interact with the PC with the same strength.

4. Comparison between simulation and experimental result

Computationally, the extraction efficiency increases gradually with the etch-depth until it reaches the MQWs. For comparison purposes, various PC LEDs of different etch-depths were fabricated. The other critical parameters such as lattice constants ($a\sim 1200\text{nm}$) and filling-factors ($f\sim 0.20$) were fixed. Generally, the large filling factor leads to the high extraction-efficiency. We could observe the same tendency till the filling-factor approached around 0.20. However, when the filling-factor was even larger than this value, electrical properties become deteriorated. We attribute this fact to the increase of the lateral resistance. We also prepared a normal LED without nanopatterns on the same wafer as a reference. Before encapsulation, we examined the performance of the device *as is*. For the shallow-etched PC LED, the near-field pattern looks uniform over the whole surface except the electrodes [Fig. 3(a)]. On the other hand, for the device etched deeper than the MQWs, almost no light emission is observed indicating the strong non-radiative recombination.

Before measuring current-voltage (I - V) characteristic curves and light-output power, all LED devices were mounted *p*-side-up on the lead frame and molded in epoxy resin. The refractive index of epoxy resin is about 1.4. Figure 3(b) shows the change of the relative enhancement in light output as a function of etch-depth. The light output was measured by a conventional integration sphere to collect the omnidirectional radiation over whole emission wavelength. The center wavelength of the GaN LED is 457nm and its spectral width is 26nm (as a FWHM). The maximum relative enhancement of $\sim 25\%$ (averaged by ten samples) is recorded when the etch depth is 140nm, at a standard current of 20mA. Unexpectedly, the extraction efficiency decreases at the etch depth of 190nm. This decrease is partly attributed to the resistance increase resulting from the reduction of *p*-GaN volume. Experimentally, the resistance increases from 11 Ω for 140nm *p*-GaN etch-depth to 15 Ω for 200nm *p*-GaN etch-depth. The light output was measured by a conventional integration-sphere setup to collect the omnidirectional radiation. For the same sample, the relative enhancement measured at the normal direction before encapsulation was $\sim 85\%$. The relative enhancement after encapsulation is smaller because of the reduction of the index contrast and the contribution of the horizontal radiation to the light output. For samples etched deeper than the QW depth, the enhancement becomes rather smaller owing to the nonradiative recombination.

The entire L-I characteristics of the PC LED exhibiting the maximum enhancement are shown in Fig 4(a). Up to 100mA, the PC LED maintains significant improvement in light output, proving its robustness even at such a high current. Finally, we measured I - V characteristics to determine the operation voltage (V_{op}) in the LED. The forward operation voltage is unchanged and the slope of the PC LED is also similar to that of the conventional LED [Fig. 4(b)]. Therefore, the incorporation of PCs with moderate etch-depth was hardly detrimental to its electrical properties. However, the LED device with PC patterns etched

deeper than the QWs did not follow the normal I-V characteristic curve and we could not define a definite V_{op} .

Conclusion

We fabricated various PC GaN-based LEDs with different etch-depths by NIL techniques and measured the relative enhancement in the light output. The NIL technique was used to generate wide-area, high-throughput PC patterns. According to the 3D-FDTD simulation, the extraction-efficiency of the PC LED increases steadily with the etch-depth. However, the increment is reduced as the etch-depth becomes larger than $\sim\lambda/n$. In the experiment, the maximum enhancement ($\sim 25\%$) was obtained at the condition that the p -GaN layer was etched to 140nm. As seen from the I - V characteristic curve, it is worth pointing out that the enhancement was achieved without sacrificing the electrical properties. We expect that further optimization of PC parameters such as the lattice constant and the filling-factor will promise the brighter GaN LEDs.

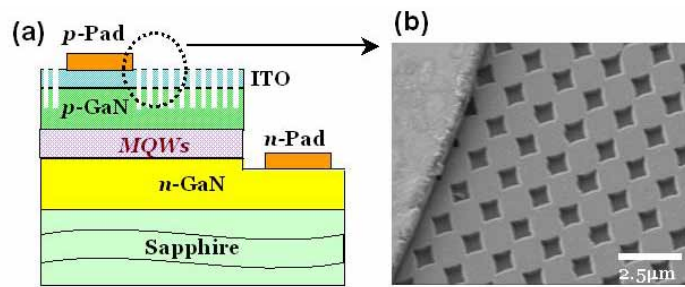


Fig. 1. (a). Schematic of a photonic-crystal (PC) GaN-based LED. The PC patterns are employed on the top surface of the GaN LED. (b) Top-view scanning electron microscope (SEM) image of a nanoimprinted PC GaN-LED. The lattice constant (a) is 1200nm and the radius of holes are $0.25a$.

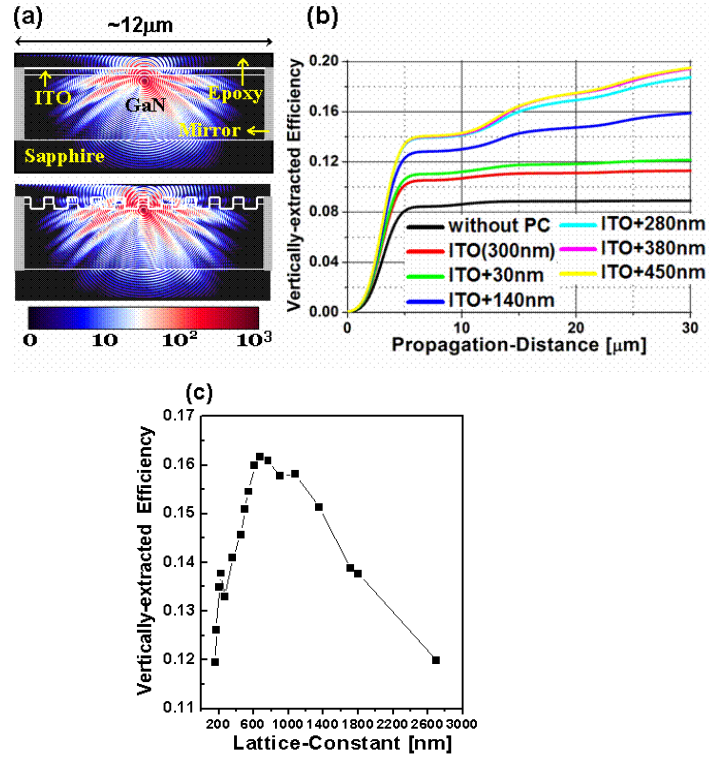


Fig. 2. (a). Snap shots of the calculated electric-field distribution of the GaN LED without PC (top) and with PC (bottom). The gray bars at the side edges represent perfect-mirrors with reflectance of 100%. Particularly, the thickness of the sapphire substrate is shrunk down to $1.5\mu\text{m}$ because of the limited memory size. (b) The vertically-extracted efficiency of the PC GaN-LED with various etch-depths as a function of the propagation-distance. The extraction-efficiency is defined as a ratio of the energy through the top GaN surface and the total generated energy. This simulation is performed by the 3D-FDTD method. (c) The vertical extraction-efficiency as a function of the lattice constant. The extraction efficiency is an integrated value till the light propagates $30\mu\text{m}$. The etch-depths are 140nm in all cases.

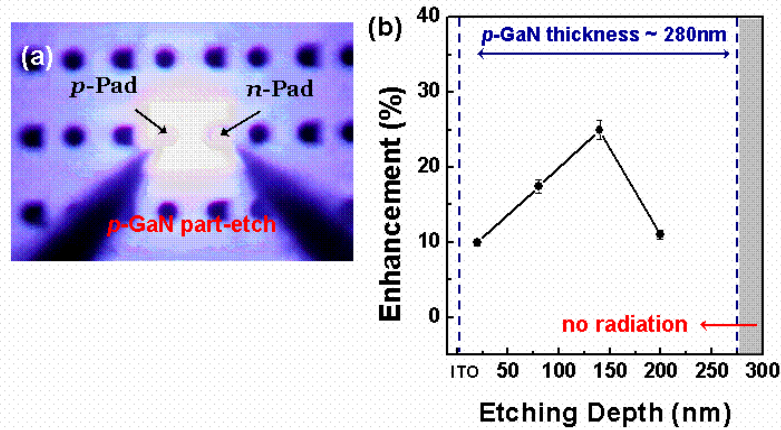


Fig. 3. (a). A typical near-field image for shallow-etched (*p*-GaN 140nm-etch) PC GaN-LED. It shows the uniform radiation over the whole surface. (b) The measured relative-enhancement as a function of etch-depth. When the device is etched deeper than the MQWs, almost no light emission is observed.

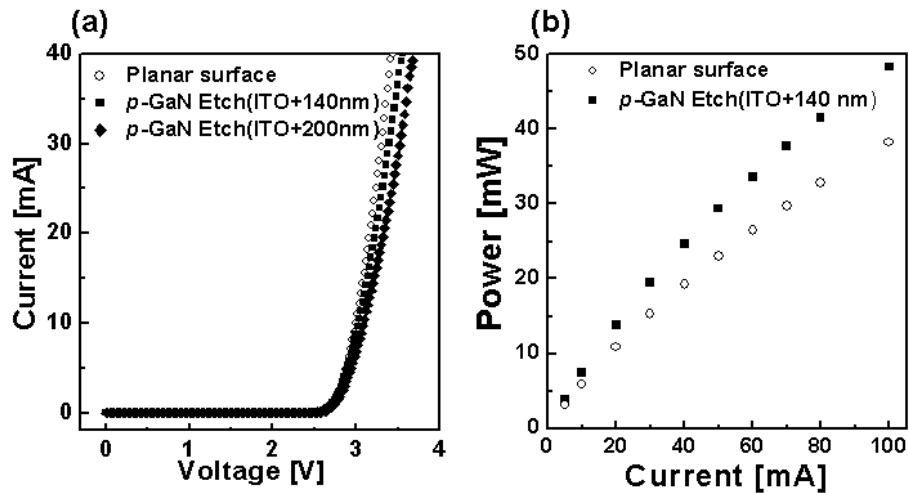


Fig. 4. (a). The entire *I*-*I* characteristics of the normal LED (unfilled circles) and the PC LED for 140nm etch-depth of *p*-GaN (filled squares) and the PC LED for 200nm etch-depth of *p*-GaN (filled diamonds). The relative enhancement of PC LED is 25% at a standard current of 20mA. (b) *I*-*V* characteristics of the normal LED (unfilled circles) and the PC LED (filled squares). For the *p*-GaN 140-nm-etched device, the electrical properties (V_{op} , slope) are hardly changed.